XPR1 Mediates the Pancreatic β-Cell Phosphate Flush

Christopher J. Barker,[1] Fernando Henrique Galvão Tessaro,[1,2] Sabrina de Souza Ferreira,[1,2] Rafael Simas,[1] Thais S. Ayala,[1,2] Martin Köhler,[1] Subu Surendran Rajasekaran,[1] Joilson O. Martins,[2] Elisabetta Darè,[1] and Per-Olof Berggren[1]

Diabetes 2021;70:111–118 | https://doi.org/10.2337/db19-0633

Glucose-stimulated insulin secretion is the hallmark of the pancreatic β-cell, a critical player in the regulation of blood glucose concentration. In 1974, the remarkable observation was made that an efflux of intracellular inorganic phosphate (P_i) accompanied the events of stimulated insulin secretion. The mechanism behind this "phosphate flush," its association with insulin secretion, and its regulation have since then remained a mystery. We recapitulated the phosphate flush in the MIN6m9 β-cell line and pseudoislets. We demonstrated that knockdown of XPR1, a phosphate transporter present in MIN6m9 cells and pancreatic islets, prevented this flush. Concomitantly, XPR1 silencing led to intracellular P_i accumulation and a potential impact on Ca^{2+} signaling. XPR1 knockdown slightly blunted first-phase glucose-stimulated insulin secretion in MIN6m9 cells, but had no significant impact on pseudoislet secretion. In keeping with other cell types, basal P_i efflux was stimulated by inositol pyrophosphates, and basal intracellular P_i accumulated following knockdown of inositol hexakisphosphate kinases. However, the glucose-driven phosphate flush occurred despite inositol pyrophosphate depletion. Finally, while it is unlikely that XPR1 directly affects exocytosis, it may protect Ca^{2+} signaling. Thus, we have revealed XPR1 as the missing mediator of the phosphate flush, shedding light on a 45-year-old mystery.

Glucose-stimulated insulin secretion is the central function of the pancreatic β-cell for which loss or malfunction contributes to type 1 and type 2 diabetes, respectively. An observation made more than 40 years ago by Freinkel et al. (1) and confirmed in several further studies (2) was that this glucose-stimulated release of insulin was accompanied by an efflux of [^{32}P]-labeled inorganic phosphate (P_i) in pancreatic islets prelabeled with [^{32}P]P_i. This "phosphate flush" was shown to be specific to pancreatic β-cells (3) and did not occur in other islet cells or the exocrine pancreas (3). The efflux occurred simultaneously with first-phase insulin release (1) but was not driven by the Ca^{2+} influx that accompanies insulin secretion (1,2). It was a dose-dependent phenomenon (4) and specific for D- over L-glucose (5) but could be promoted by a number of other insulin secretagogues (2). The source of this P_i was identified as existing under the plasma membrane (6). Over the last 45 years, there have been a number of proposals advanced to explain the phosphate flush but the presumed P_i transporter mediating this effect has not been identified, and thus, there are many unresolved questions surrounding this phenomenon. P_i metabolism has specific importance in pancreatic β-cells, as P_i is required for glycolysis and thus the operation of the β-cell as a glucose sensor (7). Furthermore, plasma buildup of P_i in, for example, chronic kidney disease could be detrimental to β-cell viability (8). Thus, the control of P_i is of central importance to the β-cell's ability to maintain blood glucose homeostasis.

Studies in plants have revealed that a number of different P_i transporters possess an SPX domain, named after proteins Syg1, Pho81, and XPR1 (9). In the mammalian genome, XPR1 is the only protein that possesses the SPX domain. XPR1 was originally characterized as a receptor for xenotropic and polytropic murine retroviruses (10). However, new studies have revealed XPR1 as the first P_i efflux transporter to be identified in metazoans (11–14). In addition, inositol pyrophosphates, which play a central role in β-cell regulation (15,16), are proposed to specifically

[1]The Rolf Luft Research Center for Diabetes and Endocrinology, Karolinska Institutet, Stockholm, Sweden

[2]Laboratory of Immunoendocrinology, Department of Clinical and Toxicological Analyses, School of Pharmaceutical Sciences, University São Paulo, São Paulo, Brazil

Corresponding author: Christopher J. Barker, chris.barker@ki.se, or Per-Olof Berggren, per-olof.berggren@ki.se

Received 9 July 2019 and accepted 17 August 2020

This article contains supplementary material online at https://doi.org/10.2337/figshare.12821192.

C.J.B. and F.H.G.T. contributed equally to this study.

See accompanying article, p. 27.

bind and activate SPX domains, including that of XPR1 (17–19). XPR1 is therefore the first potential candidate mediating the phosphate flush. Using a pancreatic β-cell line and a primary β-cell model, we tested the hypothesis that XPR1 is responsible for the phosphate flush and studied its regulation by inositol pyrophosphates. We demonstrate that XPR1 is important for the regulation of intracellular P_i in the β-cells and is indeed the missing player that mediates the phosphate flush.

RESEARCH DESIGN AND METHODS

All animal experiments were approved by the Animal Ethics Committee of Northern Stockholm, Sweden, and carried out in accordance with the National Institutes of Health's *Guide for the Care and Use of Laboratory Animals*.

Materials

Cell culture reagents, Hanks' balanced salt solution, M-PER Mammalian Protein Extraction Reagent, Pierce BCA Protein Assay, Lipofectamine 2000 and RNAiMAX, TaqMan gene expression assays, and siRNAs were obtained from Thermo Fisher Scientific (Stockholm, Sweden). Silencing was implemented by IP6K siRNAs (15,16) or XPR1 siRNAs (identification numbers s72989 and s201933) with silencer select negative control 1 (catalog number 4390843). Common chemicals, Accutase, and N2-(*m*-Trifluorobenzyl), N6-(p-nitrobenzyl) purine (TNP) were from Sigma-Aldrich (Stockholm, Sweden) or Merck KGaA (Darmstadt, Germany). Carrier-free [^{32}P]orthophosphate and the insulin AlphaLISA assay were obtained from PerkinElmer (Stockholm, Sweden). PiColorLock malachite green–based P_i assay was obtained from Expedeon/Abcam (Cambridge, U.K.).

Cell Culture and RNA Silencing in MIN6m9 Cells

MIN6m9 cells (20) were cultured in complete DMEM and silenced 24 h after seeding as described previously (15,16).

Preparation and RNA Silencing of Pseudoislets

Islets were isolated by collagenase digestion from the pancreata of male C57BL/6J mice and immediately extracted for RNA analysis or cultured in complete RPMI medium with 10% FBS (16). The following day, the islets were washed with Hanks' balanced salt solution and dissociated into cells using 100 μL Accutase/tube containing ∼200 islets in a ThermoMixer shaker (Eppendorf, Göteborg, Sweden) at 500 rpm and 37°C for 10 min, followed by gentle pipetting. Then, fresh Accutase (200 μL) was added, and the step was repeated. Cells were transferred by centrifugation (180*g* for 8 min) to complete DMEM without antibiotics and counted. The siRNAs were premixed with Lipofectamine RNAiMAX in Opti-MEM for 5 min. This was added to the cell suspension (10-fold dilution). After 5 min, the cell suspension was distributed (200 μL/well) into PerkinElmer CellCarrier Spheroid ULA 96-well microplates (2,500 cells, 10 pmol siRNAs, and 0.6 μL RNAiMAX in each well). After plate centrifugation (180*g* for 6 min), cells were allowed to reaggregate into three-dimensional structures (∼1 pseudoislet/well) for ∼5 days in a cell-culture incubator.

RNA Extraction and Real-time RT-PCR

Total RNAs were extracted from MIN6m9 cells, islets, or pseudoislets (RNeasy Mini and Micro kits; Qiagen, Sollentuna, Sweden) and reverse transcribed as previously described (15,16). The relative expression of mRNA was measured by real-time RT-PCR TaqMan Gene Expression Assays: XPR1 (Mm00495501_m1), IP6K1 (Mm00501996_m1), and IP6K2 (Mm01232057_m1) using ABI 7300 instrument and QuantStudio 5 (Thermo Fisher Scientific). 18S rRNA (TaqMan rRNA Control Reagent) was used as endogenous control.

Dynamic Incubation Assay

MIN6m9 cells were incubated at 37°C in dynamic assays as described previously (16) in order to determine either P_i efflux or insulin secretion (see detailed protocols in Supplementary Fig. 1*A*). The cells were incubated for 90 min with 25–50 μCi carrier-free [^{32}P]P_i (for P_i efflux measurements) or without this label (for measurements of insulin secretion) in modified Krebs buffer containing 5.5 mmol/L glucose. After additional 60 min in unlabeled Krebs buffer with 0.5 mmol/L glucose, the cell monolayers were subjected to the dynamic phase, exchanging buffer every minute. The radioactivity of the collected dynamic assay samples and the total cellular material was determined using a liquid scintillation counter. Insulin was determined by the AlphaLISA assay and normalized with total protein, extracted using M-PER Mammalian Protein Extraction Reagent, and determined by the BCA Protein Assay. For determining the intracellular P_i content, cells were extracted with 5% perchloric acid (PCA) at the time point indicated in Supplementary Fig. 1*B*.

Static Incubation Assay

For the determination of P_i efflux, pseudoislets were incubated at 37°C in a similar regimen as the MIN6m9 cells in the presence of [^{32}P]P_i in modified Krebs buffer with 5.5 mmol/L glucose for 90 min. [^{32}P]P_i was omitted in the experiments for measuring insulin secretion and intracellular P_i (see protocol in Supplementary Fig. 1*C*). After 50 min in 3 mmol/L glucose, the pseudoislets were subjected to the static incubation phase (i.e., basal incubation at 3 mmol/L glucose for 10 min followed by stimulation with 16.7 mmol/L glucose for 10 min). [^{32}P]P_i and insulin were determined in the samples by scintillation counting and the AlphaLISA assay, respectively. PCA extraction of the pseudoislets was performed to obtain both total intracellular P_i and cellular protein.

Measurements of Intracellular P_i

Intracellular P_i was PCA extracted from cells or pseudoislets by modifying an existing procedure (18) to recover the cellular protein (Supplementary Fig. 1*B* and *C*). Measurements of P_i were carried out using the PiColorLock assay

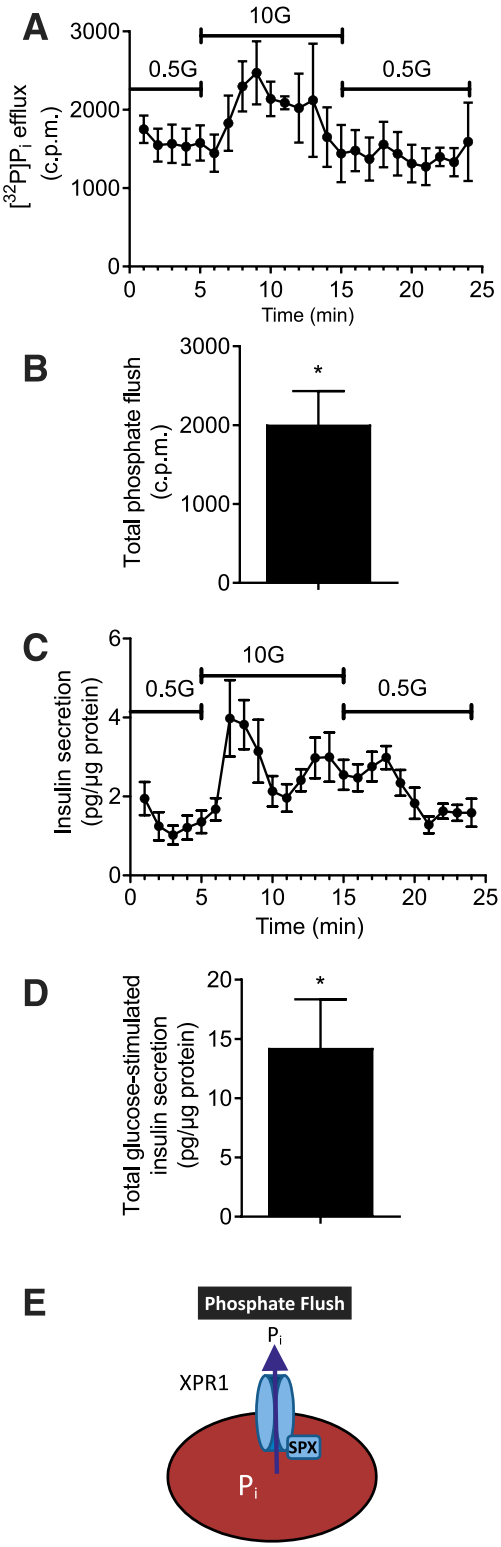

Figure 1—Determination of the phosphate flush and of insulin secretion in the pancreatic MIN6m9 β-cells. *A*: Cells were first labeled for 90 min with 25–50 μCi of carrier-free [^{32}P]P_i in a modified Krebs buffer containing 5.5 mmol/L glucose and then preincubated in Krebs buffer with 0.5 mmol/L glucose for 1 h. Next, this buffer was exchanged, every minute, for 30 min, followed by stimulation with 10 mmol/L glucose at the time indicated, again exchanging solution every minute. Samples, consisting of the exchanged buffer, were collected from the final 5 min of the basal glucose (0.5 mmol/L) to the end of the experiment, and their radioactivity was determined in a scintillation counter. A more detailed protocol is available in Supplementary Fig. 1*A*. Data are means ± SEM; $n = 4$. *B*: Quantification of the total glucose-stimulated phosphate efflux in *A* was obtained by initially averaging the first five points of each experiment (1–5 min, basal glucose). This value was then subtracted from each of the 10 points (6–15 min) under glucose stimulation. The resulting values were then added together; means ± SEM; $n = 3$. *$P < 0.05$, one-sample *t* test. *C*: In parallel experiments to the one on phosphate flush shown in *A*, samples were taken for measurement of insulin secretion. Data are means ± SEM; $n = 6$. *D*: Quantification of the total glucose-stimulated insulin release in experiment shown in *C* was obtained by subtracting the average basal insulin secretion in each experiment (1–5 min) from the insulin secretion under 10-min glucose stimulation, as described for phosphate efflux; means ± SEM; $n = 6$. *$P < 0.05$, one-sample *t* test. The *n* value denotes number of independent experiments. *E*: Illustration hypothesizing the potential role of XPR1 in β-cell phosphate flush. The SPX domain is proposed to have a regulatory function. 0.5G, 0.5 mmol/L glucose; 10G, 10 mmol/L glucose; c.p.m., counts per minute.

and total protein was determined by the BCA Protein Assay.

Measurements of Intracellular Free Calcium Concentrations

Pseudoislets were loaded with 2 μmol/L Fura-2 LeakRes (AM) (TEFLabs, Inc., Austin, TX) in modified Krebs buffer containing 3 mmol/L glucose for 60 min. After loading, a single pseudoislet was transferred to an open perifusion chamber maintained at 37°C. The pseudoislet was perifused with Krebs buffer containing 3 mmol/L glucose and 16.7 mmol/L glucose was used for stimulation. Intracellular free calcium concentration ($[Ca^{2+}]_i$) was measured as the 340/380 nm fluorescence ratio using a Spex Fluorolog spectrophotometer coupled to a Zeiss Axiovert 35M microscope with a Zeiss Fluar 40×/1.30 oil immersion objective (Carl Zeiss, Göttingen, Germany).

Statistical Analysis

The data, expressed as means ± SEM, were statistically analyzed with GraphPad Prism software version 5.0. Details of analyses are indicated in figure legends, text, and Supplementary Table 1.

Data and Resource Availability

The data sets generated during and/or analyzed during the current study are available from the corresponding authors on reasonable request.

RESULTS AND DISCUSSION

In the original studies, it was shown that in pancreatic islets, only the β-cells mediated the phosphate flush (3). In order to investigate this phenomenon, we sought to use a currently established glucose-responsive β-cell line from mouse (MIN6m9), as it is a more experimentally amenable system. MIN6m9 cells are a good β-cell surrogate, both in terms of their response to glucose and the regulation of

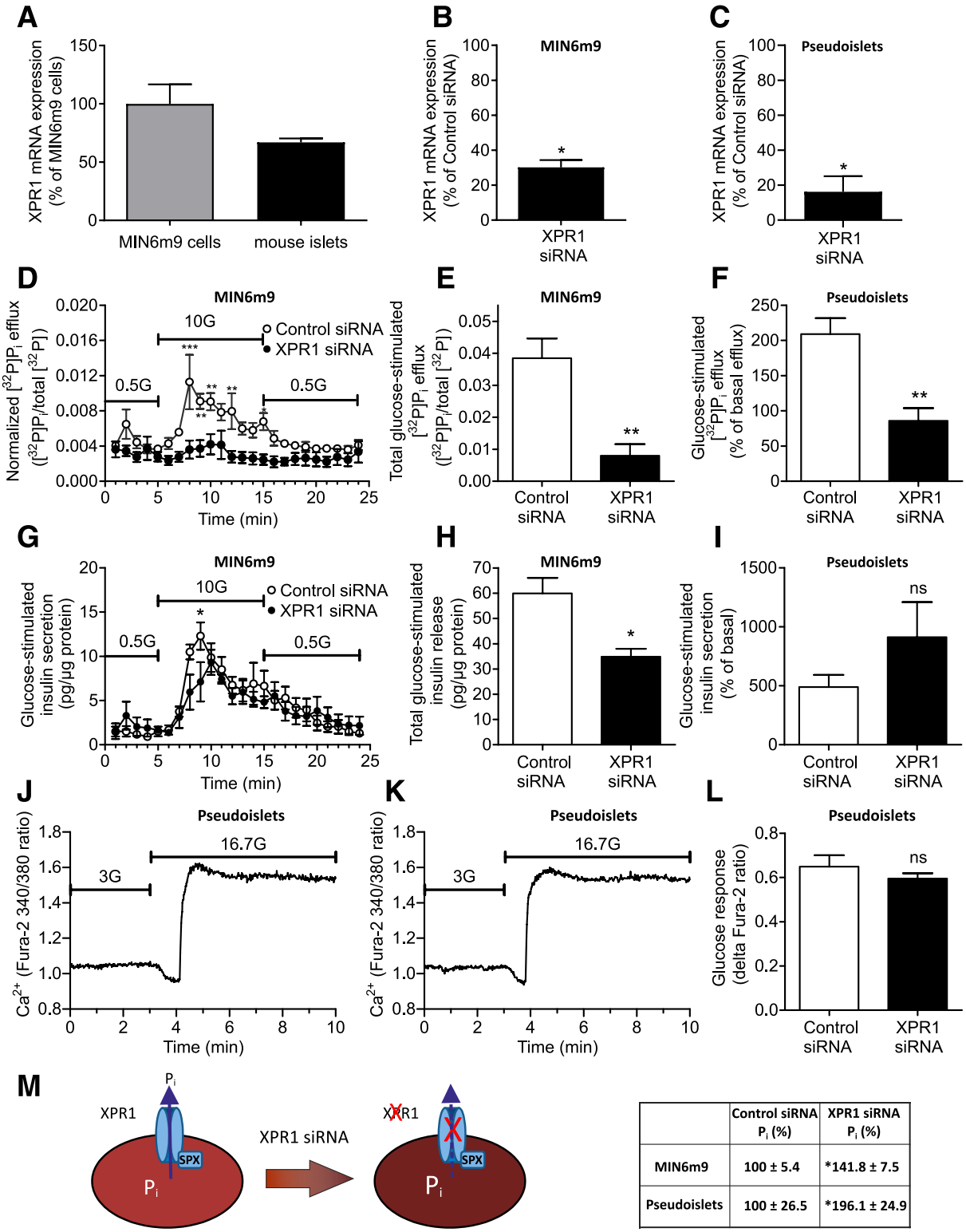

	Control siRNA P_i (%)	XPR1 siRNA P_i (%)
MIN6m9	100 ± 5.4	*141.8 ± 7.5
Pseudoislets	100 ± 26.5	*196.1 ± 24.9

Figure 2— Evaluation of the role of XPR1 in pancreatic β-cell phosphate flush, insulin secretion, and $[Ca^{2+}]_i$ responses. *A*: Expression of XPR1 mRNA in MIN6m9 cells and islets from C57BL/6J mice; means ± SEM; $n = 3$ and $n = 5$ preparations, respectively. Efficiency of XPR1 silencing in MIN6m9 cells (*B*) and C57BL/6J mouse pseudoislets (*C*) treated with siRNAs. The reduction in XPR1 mRNA is expressed as percentage relative to control siRNA; means ± SEM. *$P < 0.05$, 95% CI. Experiments in *D*, *E*, *G*, and *H* were carried out in MIN6m9 cells using the dynamic incubation protocol described in Fig. 1 and Supplementary Fig. 1*A*. *D*: Glucose-stimulated phosphate flush is lost following XPR1 knockdown. $[^{32}P]P_i$ efflux is normalized to total $[^{32}P]$ in dish; means ± SEM; $n = 4$. *$P < 0.05$, **$P < 0.01$, ***$P < 0.001$, two-way ANOVA with Bonferroni post-test (see Supplementary Table 1). Note: a reduction in $[^{32}P]P_i$ efflux with XPR1 knockdown is apparent under basal conditions if basal values are normalized to protein: control siRNA, 5.8 ± 1.3 counts per minute (cpm)/µg; XPR1 siRNA, 2.0 ± 0.65 cpm/µg; means ± SEM; $n = 4$. $P < 0.05$, Student *t* test. *E*: Quantification of the total phosphate flush under glucose stimulation in XPR1 siRNA–treated cells vs. control siRNA-treated cells in *D*; means ± SEM; $n = 4$. **$P < 0.01$, Student *t* test (for the calculations, see Fig. 1*B*). *F*:

exocytosis (16,21). We first determined that the phosphate flush occurred in this cell model. Thus, we prelabeled MIN6m9 cells with carrier-free $[^{32}P]P_i$ using similar protocols to the original studies in islets (1). This was followed by a dynamic incubation assay (16,21) that allows us to assess temporal changes in P_i release and insulin secretion in response to glucose with a 1-min time resolution (Supplementary Fig. 1*A*). Figure 1*A* and *B* illustrate that glucose stimulation of these cells leads to the expected enhanced efflux of $[^{32}P]P_i$, as well as to an increase in insulin secretion (Fig. 1*C* and *D*).

Intracellular P_i in the MIN6m9 cells cultured in complete DMEM was 41.3 ± 1.9 pmol P_i/μg protein (mean ± SEM; $n = 6$), which is comparable to other cells (18,19). However, it has been reported that intracellular P_i accumulates during the low-glucose condition used to achieve basal insulin secretion (22). Under these settings (Supplementary Fig. 1*B*), we also observed an accumulation of P_i (107.7 ± 13.0 pmol P_i/μg protein; $n = 6$). This accumulation was significantly reduced (50.9 ± 16.1%; $n = 6$; $P < 0.05$, one-sample *t* test) by maintaining high glucose (10 mmol/L) during the preincubation period. Thus, the phosphate flush is a possible mechanism normalizing intracellular P_i during glucose stimulation to avoid reaching very high levels associated with β-cell dysfunction (8).

We hypothesized that XPR1 plays a crucial role in P_i efflux in β-cells, mediating the phosphate flush (Fig. 1*E*). We detected XPR1 mRNA expression in both MIN6m9 cells and mouse pancreatic islets (Fig. 2*A*). We then used siRNA silencing to knockdown the expression of XPR1 in MIN6m9 cells to ~30% of its normal level (Fig. 2*B*). This treatment did not affect either the cell number or the cell viability (Supplementary Fig. 2). We then used the dynamic assay to assess the effect of silencing XPR1 on the phosphate flush. In this case, we normalized the P_i efflux to the total phosphate in the cells in order to control for any disturbance to phosphate metabolism mediated by the silencing. Figure 2*D* and *E* show that knockdown of XPR1 dramatically reduced the glucose-stimulated P_i efflux to ~10% of the control value. Normalizing P_i efflux to protein revealed that XPR1 also significantly impacted basal P_i efflux (Fig. 2, legend). We then used pseudoislets, a primary β-cell model in which we exploited the siRNA approach and reached a similar level of XPR1 knockdown as in MIN6m9 cells (Fig. 2*C*). A consequent reduction of the phosphate flush was observed (Fig. 2*F*). Consistent with the decrease in P_i efflux, intracellular P_i concentrations were significantly enhanced upon XPR1 silencing, both in MIN6m9 cells and pseudoislets (Fig. 2*M*). Thus, XPR1 is responsible for the β-cell glucose-stimulated phosphate flush.

An important question, unresolved in previous studies (2), is whether or not the phosphate flush is necessary for insulin secretion or is simply a parallel phenomenon that accompanies exocytosis. Indirect evidence suggested that the two processes could be disassociated. For example, removal of extracellular Ca^{2+} or blockade of its entry prevents insulin release but not the phosphate flush (1,2). Conversely, stimulation of secretion by sulphonylureas does not increase the phosphate flush (7). With the identification of XPR1 as the mediator of the flush, we could, for the first time, test directly the relationship between the phosphate flush and insulin exocytosis. Using identical conditions to those used to assess the phosphate flush, we measured the impact of XPR1 silencing on insulin release. Figure 2*G* and *H* show only a modest impact on first-phase insulin secretion under conditions in which the phosphate flush is almost ablated in MIN6m9 cells. XPR1 knockdown in pseudoislets did not significantly impact the five-fold increase in insulin secretion provoked by 10 min of glucose stimulation (Fig. 2*I*). Taken together, these data suggest that the XPR1-mediated phosphate flush is not essential for insulin secretion.

Freinkel (2) originally proposed that an interaction between Ca^{2+} ions and the phosphate flush could contribute to biphasic insulin secretion. Interestingly, several reports have highlighted the relationship of XPR1-mediated P_i efflux to cellular calcium metabolism (12–14), including calcification due to P_i buildup and calcium phosphate precipitation (13,14). We therefore examined the glucose-induced changes in $[Ca^{2+}]_i$ in pseudoislets in which XPR1 was knocked down (Fig. 2*J* and *K*). If XPR1 was preventing calcium phosphate precipitation, we might anticipate a blunted $[Ca^{2+}]_i$ response in its absence. There was no

Glucose-stimulated phosphate flush is reduced in pseudoislets following XPR1 knockdown in comparison with control siRNA–treated pseudoislets; means ± SEM; $n = 4$. $^{**}P < 0.01$, Student *t* test. *G*: The effect of XPR1 knockdown on glucose-stimulated insulin release was assessed in parallel experiments to the one in *D* and *E*; means ± SEM; $n = 4$, two-way ANOVA. $^{*}P < 0.05$ with Bonferroni post-test (Supplementary Table 1). *H*: Quantification of total insulin secretion under glucose stimulation in the experiment shown in *G*; means ± SEM; $n = 4$. $^{*}P < 0.05$, Student *t* test (for the calculations, see Fig. 1*D*). *I*: Glucose-stimulated insulin release is not significantly affected following XPR1 knockdown in pseudoislets. Insulin secretion induced by stimulation with 16.7 mmol/L glucose for 10 min is expressed as percentage of basal secretion at 3 mmol/L glucose for 10 min. Basal secretion was also unaffected by XPR1 silencing (control siRNA, 38.6 ± 3.3, XPR1 siRNA, 41.6 ± 10.1 insulin secretion, pg/μg protein). Data are means ± SEM; $n = 5$; P = NS, Student *t* test. *J–L*: Impact of XPR1 knockdown on glucose-stimulated increases in $[Ca^{2+}]_i$ in pseudoislets. *J*: Example of $[Ca^{2+}]_i$ trace of control siRNA–treated pseudoislets. *K*: Example of $[Ca^{2+}]_i$ trace of XPR1 siRNA–treated pseudoislets. *L*: Quantification of glucose-stimulated increases in $[Ca^{2+}]_i$, expressed as delta change in Fura-2 340/380 ratio, in control siRNA–treated pseudoislets vs. XPR1 siRNA–treated pseudoislets; $n = 6–7$; P = NS, Student *t* test. *M*: Impact of XPR1 knockdown on total intracellular P_i, which was determined with the PiColorLock assay in MIN6m9 cells or pseudoislets at the time points indicated in Supplementary Fig. 1*B* and *C*. Data are expressed as percentage of the corresponding control siRNA after normalization to total protein; means ± SEM; $n = 3$ (MIN6m9 cells) or $n = 5$ (pseudoislets). $^{*}P < 0.05$, Student *t* test. The *n* value denotes number of independent experiments. 0.5G, 0.5 mmol/L glucose; 3G, 3 mmol/L glucose; 10G, 10 mmol/L glucose; 16.7G, 16.7 mmol/L glucose.

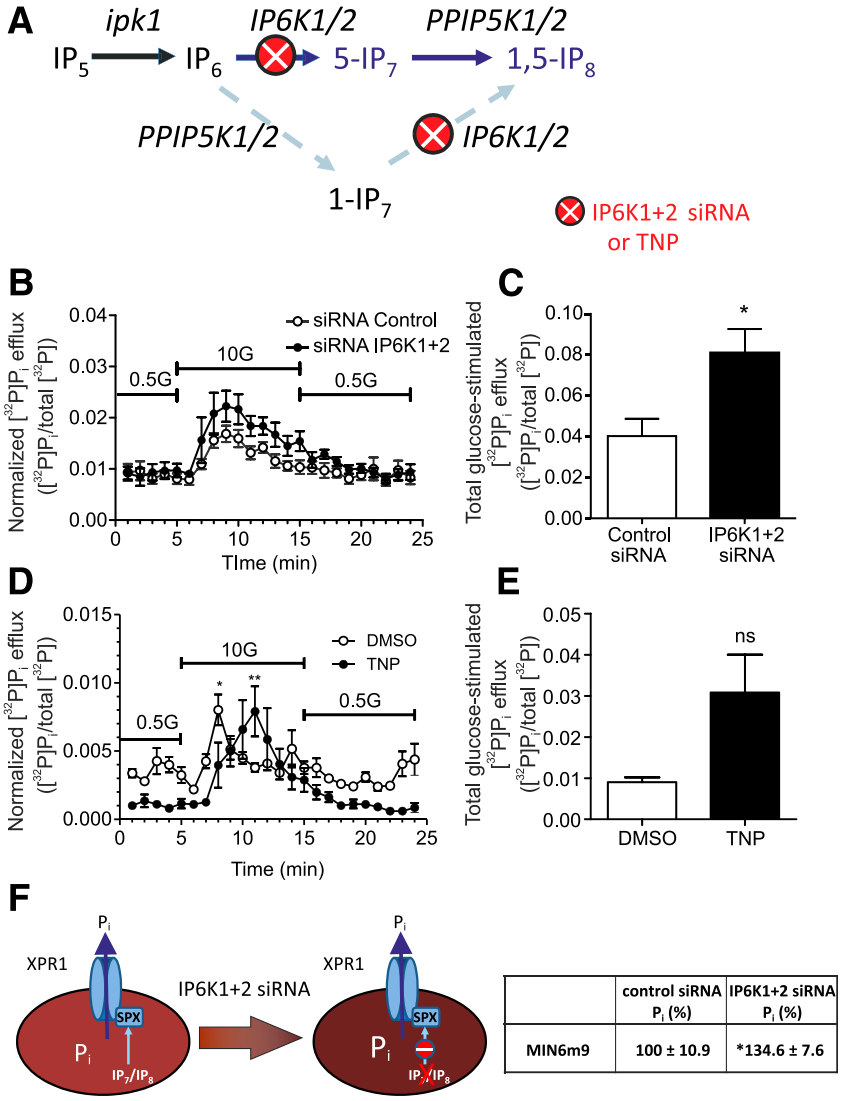

	control siRNA P_i (%)	IP6K1+2 siRNA P_i (%)
MIN6m9	100 ± 10.9	*134.6 ± 7.6

Figure 3— Phosphate efflux is regulated by inositol pyrophosphates. *A*: Scheme illustrating the formation of inositol pyrophosphates and the use of either siRNA or the pharmacological pan-IP6K inhibitor, TNP, to reduce inositol pyrophosphate formation. *B*: Impact of combined siRNA knockdown of IP6K1 and IP6K2 on phosphate flush compared with control siRNA in MIN6m9 cells. $[^{32}P]P_i$ efflux is normalized to total $[^{32}P]$ in dish; means ± SEM; $n = 4$, (there was an overall significant impact on phosphate efflux when IP6K1 and IP6K2 were knocked down. ***$P < 0.0001$, two-way ANOVA, Supplementary Table 1). *C*: Quantification of total phosphate flush under glucose stimulation in IP6K1 and IP6K2 siRNA-treated cells and controls in the experiments illustrated in *B*. There was an overall significant increase in phosphate flush following IP6K1 and IP6K2 knockdown; means ± SEM; $n = 4$. *$P < 0.05$, Student *t* test (for calculations, see Fig. 1*B*). *D*: Impact of TNP or vehicle (DMSO) on phosphate flush in MIN6m9 cells. The inhibitor TNP, or vehicle, was added for the last 30 min of the preincubation and during the subsequent steps. $[^{32}P]P_i$ efflux is normalized to total $[^{32}P]$ in dish, (there was an overall significant impact of TNP on phosphate efflux. ***$P < 0.0001$, two-way ANOVA, with significant differences at two distinct times; means ± 6 SEM; $n = 4$. *$P < 0.05$, **$P < 0.01$, Bonferroni post-test, Supplementary Table 1). To quantify impact of TNP on basal secretion, the first five basal points of the dynamic protocol were averaged for each experiment ($[^{32}P]P_i$/total $[^{32}P]$): DMSO, 0.0036 ± 0.00027; TNP, 0.0011 ± 0.00023; means ± SEM; $n = 4$. $P < 0.0005$, Student *t* test. *E*: Quantification of total phosphate efflux under glucose stimulation in TNP- and DMSO-treated cells in the experiments showed in *D*; means ± SEM; $n = 4$. P = NS, Student *t* test (for calculations, see Fig. 1*B*). *F*: Impact of IP6K1+2 knockdown on total intracellular P_i, which was determined with the PiColorLock assay in MIN6m9 cells at the time points indicated in Supplementary Fig. 1*B*. Data are expressed as percentage of the corresponding control siRNA after normalization to total protein; means ± SEM; $n = 6$. *$P < 0.05$, Student *t* test. The *n* value denotes number of independent experiments. 0.5G, 0.5 mmol/L glucose; 10G, 10 mmol/L glucose.

significant impact on the glucose-stimulated Ca^{2+} transient of XPR1 knocked down pseudoislets compared with controls (Fig. 2*J–L*). However, a subsequent stimulation by 25 mmol/L potassium, which drives a higher peak increase in $[Ca^{2+}]_i$, led to a significantly reduced increase in $[Ca^{2+}]_i$ in the XPR1 knocked down pseudoislets (Δ Fura-2 ratio; control siRNA–treated, 0.716 ± 0.049; XPR1 siRNA–treated, 0.544 ± 0.022, means ± SEM; $n = 6–7$; $P < 0.05$, Student *t* test). These data suggest that under superphysiological conditions or prolonged stimulation, the XPR1-mediated phosphate flush could serve to prevent calcium phosphate precipitation also in pancreatic β-cells, thus protecting the

integrity of $[Ca^{2+}]_i$ signaling, a key driving force of insulin exocytosis (23,24).

The SPX domain found in XPR1 is regulatory and not necessary for P_i transport (9,17). Since inositol derivatives and particularly the inositol pyrophosphates (17) can specifically bind to SPX domains, it is possible that they regulate the phosphate flush through this domain (9,17). We therefore investigated whether inositol pyrophosphates have any role in the regulation of the phosphate flush in MIN6m9 cells, a good β-cell model in studies on inositol pyrophosphates (15,16). We used two complementary approaches to curtail the production of the critical inositol pyrophosphates, 5-diphosphoinositol pentakisphosphate (5-PPIP$_5$/5-IP$_7$) and 1,5-bisdiphosphoinositol tetrakisphosphate (IP$_8$) (Fig. 3*A*).

Firstly, we used siRNA to knock down the two IP6Ks that exist in pancreatic β-cells (IP6K1 and IP6K2) (15,16). This prevents the production of 5-IP$_7$ and thus also the formation of IP$_8$ (Fig. 3*A*). Under these conditions, IP6K1 and IP6K2 are knocked down by ~40% and 50%, respectively, which leads to a 75% reduction in IP$_7$ (15) (Supplementary Fig. 3*A* and *B*). Again, we applied the dynamic protocol to study the P_i efflux. Reduction in the levels of IP6K1 and IP6K2 caused a significantly increased glucose-induced phosphate flush, without affecting basal P_i efflux (Fig. 3*B* and *C*). However, under these conditions, the expression of XPR1 mRNA was doubled (Supplementary Fig. 4), suggesting a compensatory mechanism for the loss of the stimulatory inositol pyrophosphates. In addition, there was an accumulation of intracellular P_i (Fig. 3*F*), as reported in other cells in which IP6Ks were knocked down (18).

We also used a short-term pharmacological approach applying the pan-specific IP6K inhibitor TNP to circumvent the longer-term adaptive responses seen above. This too blocks the formation of both 5-IP$_7$ and IP$_8$ (Fig. 3*A*). In contrast to the long-term knockdown of IP6Ks, TNP reduced P_i efflux under basal conditions and delayed the phosphate flush rise (Fig. 3*D* and legend). These data show that acute knockdown of 5-IP$_7$ and IP$_8$ production inhibits basal phosphate efflux via XPR1, consistent with two recent reports in other cells (18,19). However, TNP treatment does not reduce the glucose-stimulated phosphate flush (Fig. 3*D* and *E*). It is possible that the acute TNP treatment leads to a short-term compensatory adaption by which more existing XPR1 is translocated to the plasma membrane of β-cells, as observed for active K_{ATP} membrane channels upon glucose stimulation (25). Another factor that could alter P_i efflux kinetics is the buildup of intracellular P_i that we (Fig. 3*F*) and others (18) observe on IP6K knockdown. Furthermore, while our strategy reduces 5-IP$_7$ and IP$_8$, it will not impact a glucose-generated production of 1-IP$_7$, which has recently been shown to be more potent that 5-IP$_7$ in activating XPR1 (19). Thus, we would suggest that under basal glucose conditions P_i efflux via XPR1 is directly driven by inositol pyrophosphates. However, under the glucose stimulatory conditions of the phosphate flush, other so far unidentified factors linked to glucose metabolism contribute to a more complex regulation of the XPR1-dependent P_i efflux.

Overall, our study has solved an important aspect of the β-cell phosphate flush (1). We demonstrate that XPR1 is the mediator of glucose-stimulated P_i efflux and that this process is largely independent from inositol pyrophosphate regulation. Furthermore, we show that the phosphate flush is unlikely to contribute to glucose-stimulated insulin secretion, while providing a hint that the ultimate role of this mechanism may be to prevent calcium phosphate precipitation and thus protect pancreatic β-cell Ca^{2+} signaling.

Acknowledgments. The authors thank Professor S. Seino (Kobe University Graduate School of Medicine, Kobe, Japan) for the gift of MIN6m9 cells; Dr. J.H. Park (Soonchunhyang University College of Medicine, Cheonan, Korea), Dr. B. Leibiger and Dr. V.M. Lauschke (Karolinska Institutet, Stockholm, Sweden), Professor D. Piston (Washington University School of Medicine, St. Louis), and Dr. C. Reissaus (Novo Nordisk Research Center, Indianapolis) for advice about pseudoislets; and Professor A. Saiardi and Dr. M.S. Wilson (UCL, London, UK) for advice on P_i assays.

Funding. This study was supported by the Vetenskapsrådet, the Novo Nordisk Foundation, Karolinska Institutet, the Swedish Diabetes Association, The Family Knut and Alice Wallenberg Foundation, Diabetes Research and Wellness Foundation, Stiftelsen för Strategisk Forskning, Berth von Kantzow's Foundation, The Skandia Insurance Company Ltd., Strategic Research Programme in Diabetes at Karolinska Institutet, ERC-2013-AdG (338936-Betalmage), ERC-2018-AdG (834860 EYELETS), the Stichting af Jochnick Foundation, the Family Erling-Persson Foundation, Fundação de Amparo à Pesquisa do Estado de São Paulo grants 2010/02272-0, 2014/05214-1, and 2017/11540-7, CNPq (PQ-1D) grant 301617/2016-3, and Swedish Foundation for International Cooperation in Research and Higher Education and Coordenação de Aperfeiçoamento de Pessoal de Nível Superior grants.

Duality of Interest. P.-O.B. is Chief Executive Officer of the biotech company Biocrine AB, and C.J.B. and M.K. are consultants with this company. No other potential conflicts of interest relevant to this article were reported.

Author Contributions. C.J.B. and P.-O.B. conceived the project. C.J.B., F.H.G.T., S.d.S.F., R.S., T.S.A., M.K., J.O.M., E.D., and P.-O.B. designed experiments. C.J.B., F.H.G.T., S.d.S.F., R.S., T.S.A., M.K., S.S.R., and E.D. carried out experiments. C.J.B., F.H.G.T., S.d.S.F., R.S., T.S.A., M.K., and E.D. analyzed data. C.J.B. and P.-O.B. wrote the article with input from all authors. C.J.B. and P.-O.B. are the guarantors of this work and, as such, had full access to all of the data in the study and take responsibility for the integrity of the data and the accuracy of the data analysis.

References

1. Freinkel N, Younsi CE, Bonnar J, Dawson RM. Rapid transient efflux of phosphate ions from pancreatic islets as an early action of insulin secretagogues. J Clin Invest 1974;54:1179–1189

2. Freinkel N. Phosphate translocations during secretory stimulation of pancreatic islets. Adv Exp Med Biol 1979;119:71–77

3. Bukowiecki L, Trus M, Matschinsky FM, Freinkel N. Alterations in pancreatic islet phosphate content during secretory stimulation with glucose. Biochim Biophys Acta 1979;583:370–377

4. Pierce M, Bukowiecki L, Asplund K, Freinkel N. [^{32}P] Orthophosphate efflux from pancreatic islets: graded response to glucose stimulation. Horm Metab Res 1976;8:358–361

5. Pierce M, Freinkel N. Anomeric specificity for the rapid transient efflux of phosphate ions from pancreatic islets during secretory stimulation with glucose. Biochem Biophys Res Commun 1975;63:870–874

6. Freinkel N, Pedley KC, Wooding P, Dawson RM. Localization of inorganic phosphate in the pancreatic B cell and its loss on glucose stimulation. Science 1978;201:1124–1126

7. Carpinelli AR, Malaisse WJ. The stimulus-secretion coupling in glucose-induced insulin release xliv. A possible link between glucose metabolism and phosphate flush. Diabetologia 1980;19:458–464
8. Nguyen TT, Quan X, Xu S, et al. Intracellular alkalinization by phosphate uptake via type III sodium-phosphate cotransporter participates in high-phosphate-induced mitochondrial oxidative stress and defective insulin secretion. FASEB J 2016;30:3979–3988
9. Secco D, Wang C, Arpat BA, et al. The emerging importance of the SPX domain-containing proteins in phosphate homeostasis. New Phytol 2012;193:842–851
10. Kozak CA. The mouse "xenotropic" gammaretroviruses and their XPR1 receptor. Retrovirology 2010;7:101
11. Giovannini D, Touhami J, Charnet P, Sitbon M, Battini JL. Inorganic phosphate export by the retrovirus receptor XPR1 in metazoans. Cell Rep 2013;3:1866–1873
12. Ansermet C, Moor MB, Centeno G, et al. Renal fanconi syndrome and hypophosphatemic rickets in the absence of xenotropic and polytropic retroviral receptor in the nephron. J Am Soc Nephrol 2017;28:1073–1078
13. Legati A, Giovannini D, Nicolas G, et al. Mutations in XPR1 cause primary familial brain calcification associated with altered phosphate export. Nat Genet 2015;47:579–581
14. Pimentel LF, Lemos RR, Oliveira JR. Phosphate transporters expression in patients with primary familial brain calcifications. J Mol Neurosci 2017;62:276–280
15. Illies C, Gromada J, Fiume R, et al. Requirement of inositol pyrophosphates for full exocytotic capacity in pancreatic beta cells. Science 2007;318:1299–1302
16. Rajasekaran SS, Kim J, Gaboardi GC, et al. Inositol hexakisphosphate kinase 1 is a metabolic sensor in pancreatic β-cells. Cell Signal 2018;46:120–128
17. Wild R, Gerasimaite R, Jung JY, et al. Control of eukaryotic phosphate homeostasis by inositol polyphosphate sensor domains. Science 2016;352:986–990
18. Wilson MS, Jessen HJ, Saiardi A. The inositol hexakisphosphate kinases IP6K1 and -2 regulate human cellular phosphate homeostasis, including XPR1-mediated phosphate export. J Biol Chem 2019;294:11597–11608
19. Li X, Gu C, Hostachy S, et al. Control of XPR1-dependent cellular phosphate efflux by $InsP_8$ is an exemplar for functionally-exclusive inositol pyrophosphate signaling. Proc Natl Acad Sci U S A 2020;117:3568–3574
20. Minami K, Yano H, Miki T, et al. Insulin secretion and differential gene expression in glucose-responsive and -unresponsive MIN6 sublines. Am J Physiol Endocrinol Metab 2000;279:E773–E781
21. Leibiger B, Moede T, Uhles S, et al. Insulin-feedback via PI3K-C2α activated PKBalpha/Akt1 is required for glucose-stimulated insulin secretion. FASEB J 2010;24:1824–1837
22. Papas KK, Long RC Jr., Constantinidis I, Sambanis A. Role of ATP and Pi in the mechanism of insulin secretion in the mouse insulinoma betaTC3 cell line. Biochem J 1997;326:807–814
23. Berggren PO, Arkhammar P, Islam MS, et al. Regulation of cytoplasmic free Ca2+ in insulin-secreting cells. Adv Exp Med Biol 1993;334:25–45
24. Rorsman P, Renström E. Insulin granule dynamics in pancreatic beta cells. Diabetologia 2003;46:1029–1045
25. Yang SN, Wenna ND, Yu J, et al. Glucose recruits K(ATP) channels via non-insulin-containing dense-core granules. Cell Metab 2007;6:217–228